



Contents lists available at ScienceDirect

Saudi Journal of Biological Sciences

journal homepage: www.sciencedirect.com

Original article

Pegylated Eu-enabled submicron alumina spheres as potential theranostics agent RD cell line as model



Numrah Sultan^a, Syed Mujtaba ul Hassan^{b,*}, Ahmat Khurshid^c, M. Fakhar-e-Alam^{d,*}, Faisal Shahzad^b, Attaullah Shah^e, Muhammad Atif^f, Shafiq Ahmad^g, Muhammad Tamoor Masood^h

^a Department of Nuclear Engineering (DNE), PIEAS, Islamabad, Pakistan

^b Department of Metallurgical and Materials Engineering (DMME), PIEAS, Islamabad, Pakistan

^c Biophotonic and Photomedicine Research Lab, DPAM, PIEAS, Islamabad, Pakistan

^d Department of Physics, GC University Faisalabad, 38000 Pakistan

^e National Institute of Lasers and Optronics College, Pakistan Institute of Engineering and Applied Sciences (NILOP-C, PIEAS), Nilore 45650, Islamabad, Pakistan

^f Department of Physics and Astronomy, College of Science, King Saud University, P O Box 2455, Riyadh 11451, Saudi Arabia

^g Industrial Engineering Department, College of Engineering, King Saud University, P.O. Box 800, Riyadh 11421, Saudi Arabia

^h Institute for Materials Research and Innovation, University of Bolton, Bolton, United Kingdom

ARTICLE INFO

Article history:

Received 15 July 2021

Revised 30 August 2021

Accepted 1 September 2021

Available online 8 September 2021

Keywords:

Photoluminescence

Biocompatible

Theranostic

Doping

ABSTRACT

Objectives: This study is aimed to synthesis and evaluate PEGylated Eu enabled spherical alumina submicron particles (s-Al₂O₃:Eu) for potential theranostic applications.

Methods: This study is bisected into two parts, a) synthesis of PEGylated Eu enabled spherical alumina submicron particles (s-Al₂O₃:Eu), and b) characterization of the synthesized particles to determine their efficacy for potential theranostic applications.

The synthesis of the particles involved the following steps. In the first step, s-Al₂O₃:Eu is synthesized using solvothermal synthesis. In the next step, the particles undergo post synthesis water–ethanol treatment and calcination. The surface of the synthesized s-Al₂O₃:Eu particles is then coated by PEG to increase its biocompatibility.

Once the particles are prepared, they are characterized using different techniques. The microstructure, composition and structure of the particles is characterized using SEM, EDX and XRD techniques. The detection of the functional groups is done using FTIR analysis. The photoluminescence emission spectrum of s-Al₂O₃:Eu is studied using Photoluminescence spectroscopy. And, finally, the biocompatibility is studied using MTT assay on RD cell lines.

Results: The microstructure analysis, from the micrographs obtained from SEM, shows that the spherical alumina particles have a submicron size with narrow size distribution. The compositional analysis, as per EDX, confirms the presence of Oxygen, Aluminum and Europium in the particles. While, XRD analysis of s-Al₂O₃:Eu confirms the formation of alpha alumina phase after calcination at 700 °C. Emission peaks, obtained by Photoluminescence emission spectroscopy, show that the optimum emission intensities correspond to the transition from ⁵D₀ to ⁷F_j orbital of Eu³⁺. FTIR analysis confirms the successful coating of PEG. Finally, a cell viability of more than 86% is observed when the biocompatibility of the particles is studied, using MTT assay on RD cell lines.

Abbreviations: PEG, Polyethylene glycol; SEM, Scanning electron microscope; EDX, Energy-dispersive X-ray spectroscopy; XRD, X-Ray Diffraction; FTIR, Fourier-transform infrared spectroscopy; MTT3-(4, 5-dimethylthiazol-2-yl)-2,5-diphenyltetrazolium bromide; RD, Rhabdomyosarcoma.

* Corresponding authors at: Department of Metallurgy and Material Engineering, Pakistan Institute of Engineering and Applied Sciences (PIEAS), Islamabad, Pakistan (S.M. ul Hassan) and Department of Physics, GC University Faisalabad 38000, Pakistan (M.F.-e-Alam).

E-mail addresses: mujtabanaqvi29@gmail.com (S. Mujtaba ul Hassan), fakharphy@gmail.com (M. Fakhar-e-Alam).

Peer review under responsibility of King Saud University.



<https://doi.org/10.1016/j.sjbs.2021.09.001>

1319-562X/© 2021 The Author(s). Published by Elsevier B.V. on behalf of King Saud University.

This is an open access article under the CC BY-NC-ND license (<http://creativecommons.org/licenses/by-nc-nd/4.0/>).

Conclusions: s-Al₂O₃:Eu with narrow distribution are successfully synthesized. Structural and functional characterizations support the suitability of s-Al₂O₃:Eu as potential theranostic agent.

© 2021 The Author(s). Published by Elsevier B.V. on behalf of King Saud University. This is an open access article under the CC BY-NC-ND license (<http://creativecommons.org/licenses/by-nc-nd/4.0/>).

1. Introduction

The rapid research and development in the field of nanotechnology in recent years has transformed the scientific landscape of bioimaging and drug delivery. Hence, the investigation of novel biocompatible materials for application in theranostic has become a key area of interest for scientists. A theranostic agent is the one that has the capability of therapy as well as diagnosis (Xie et al., 2010). The combination of nanoparticle-based drug delivery systems with appropriate contrast agents for application in theranostic is a promising research domain with a lot of recent developments. The desired characteristics of nanoparticles-based theranostic agents include; enhanced blood circulation time, improved specific localization for drug delivery and superior imaging characteristics for diagnosis.

Research has been conducted on several nanomaterials in order to determine their efficacy as a potential theranostic. These nanomaterials include polymeric nanomaterials, metallic nanomaterials, ceramic nanomaterials and composites (Liechty et al., 2010, Huxford et al., 2010, Paul and Sharma, 2003). All these nanomaterials have their own sets of advantages and disadvantages, which are discussed briefly as follows. Polymeric nanomaterials have low toxic effects and high biocompatibility but they have low therapeutic life, which decreases their efficiency as a theranostic agent (Kwon and Furgeson, 2007). Metallic nanomaterials have high surface area, increased bioavailability and ease of surface functionalization, which makes them a viable option for drug delivery and bioimaging. However, their inadequate biodistribution, pharmacokinetics and possible toxicity remain a challenge (Arvizo et al., 2010, Mathur et al., 2018, Singh et al., 2010). Among metallic nanomaterials, silver, gold, nickel, titanium and iron-based nanoparticles are widely used for biomedicine applications (Patra et al., 2018). Ceramic nanomaterials are a suitable option as theranostic agents because of their high mechanical strength, low biodegradability, and good stability in the harsh bioenvironment which increases their bioavailability as drug carrier. The most widely researched bio-ceramics include silica and alumina (Subhadrappa et al., 2018). Mesoporous silica has gained considerable importance, in the field of theranostic, owing to its high surface area and pore volume. It can serve as multifunctional drug carrier when combined with a suitable contrast agent (Xie et al., 2010). Despite all these benefits, its applicability to clinical use is still hindered because of the difficulty in scaling up its synthesis, under good manufacturing practices (GMP). The reproducibility of the desired silica based therapeutic agent is a challenge when dealing with a fine control of size, shape, charge and surface functionalization during large scale synthesis (Nigro et al., 2018).

Among the class of inorganic porous materials for drug delivery, anodic alumina is a promising candidate because of its controlled pore size, and uniform size distribution. It also has high surface area and chemical stability. Ceramic alumina has high biocompatibility. Hence, it is being used in orthopedic prostheses and dental implants. To develop therapeutic capabilities in anodic alumina, magnetic particles can be loaded on the pores. Iron based magnetic particles can act as T2 contrast agents for magnetic resonance (MR) imaging (Palanisamy and Wang, 2019). The initial work on anodic alumina as a drug carrier in anticancer treatment comprised of loading of Apo2L/TRAIL in the pores of anodic alumina. The drug

loading capacity of 104 µg/mg was achieved with a sustained drug release profile (Wang et al., 2014). Anodic Alumina is a promising candidate for application in drug delivery and bio imaging, but the electrochemical process used for its synthesis yields high level of chemical waste (Stepniowski and Bojar, 2011). A facile solvothermal synthesis of porous alumina is cost effective with the least chemical waste generated. Furthermore, the porous submicron alumina spheres obtained by this synthesis are found to be biocompatible with high drug loading capacity (Ali et al., 2019). It is also possible to incorporate imaging and diagnostic characteristics in a drug delivery system by doping them with suitable contrast agents. Several polymer, metallic and ceramic based theranostic agents are being explored for simultaneous application in drug delivery and imaging (Johnson et al., 2014, Luk and Zhang, 2014, Roy et al., 2003, Soica et al., 2018). Depending on the contrast agents being used, various imaging techniques are being explored and studied for diagnostic purposes, including magnetic resonance imaging (MRI), computerized tomography (CT), Fluorescence resonance energy transfer (FRET), photoluminescence imaging (PLI), positron emission tomography (PET) among others. Optical imaging like photoluminescence has different advantages like high resolution, better sensitivity, low cytotoxicity and portable instrumentation (Chen et al., 2020; Zhu et al., 2019). Rare earths (RE) doped biomarkers are well known for their sharp emissions, low cytotoxicity, and broad emission spectrum. The absorption behavior of RE dopants depend on the f-f transitions and is independent of particle size and morphology. Eu⁺³, a lanthanide based phosphors exhibits good emission properties originating from the transition between the ⁵D₀ to ⁷F_J (J = 0,1,2,3 and 4) comprising of the electric and magnetic dipole transitions at different wavelengths (Wang and Liu, 2009). The choice of a host material for doping of the rare earth doped is also critical, desired characteristics of host materials include high quantum yield, controlled emission profile, low phonon energy and lattice parameters with dimensions comparable to the dopant (Li, et al., 2009) In a study by Liu and coworkers, the doping of Eu in alpha alumina yields promising photoluminescence results. Photoluminescence properties of the Eu-doped alpha-Al₂O₃ microspheres. Moreover, PEGylated alumina is also found to be biocompatible (Ali et al., 2019). The doping of Europium in porous alumina spheres yield encouraging photoluminescence properties, that is desired in bioimaging applications, while alumina acts as a drug delivery system. This naturally directs a new spherical Eu-enabled Alumina spheres with inherent water dispersibility and biocompatibility. The study of PEGylated Eu-enabled Alumina sub-micron is a novel study in this regard. Following this theme, a novel idea has been developed to fabricate Eu doped spherical alumina with photoluminescence properties as a potential theranostic agent. The submicron capsules are inherently water dispersible and show photoluminescence characteristics with good biocompatibility.

2. Materials and Methods

2.1. Materials

Al (NO₃)₃·9H₂O and Polyethylene Glycol (PEG-4000) were obtained from Sigma Aldrich., 2- Propanol (99.5%) was procured

Merck. Glycerol (99.8%) was obtained from Fuka Chemicals. Europium Oxide (Eu_2O_3) powder was used for Eu doping.

2.2. Synthesis of PEG coated Eu doped submicron sized alumina spheres

Submicron alumina microspheres were prepared by a modified solvothermal synthesis (Saptiama et al., 2018). In a typical experiment, $\text{Al}(\text{NO}_3)_3 \cdot 9\text{H}_2\text{O}$ is added in 40 ml of 2-Propanol along with the addition of europium nitrate. After complete formation of solution, 16 ml of analytical grade glycerol was added in the mixture under vigorous stirring. The resultant solution was then placed in an autoclave at a temperature of 180 °C for 16 h. The reaction results in the formation of aluminum alkoxide. In the second stage of synthesis europium doped monodispersed glycerated aluminum was partially converted into aluminum oxide hydroxide (Bohemite) by the post synthesis water–ethanol treatment. In a typical procedure 20 mg of europium doped glycerated aluminum was mildly stirred for 48 h in a mixture of 10 ml distilled water and 10 ml ethanol. Finally, mesoporous europium doped alumina was obtained by calcination of the resultant product at a temperature of 700 °C for 2 h. PEG is then coated on the final product by stirring it in distilled water containing 20 mg of PEG. The synthesis strategy of Eu doped submicron alumina spheres is shown in Fig. 1.

2.3. Cytotoxicity evaluation on RD cell lines using MTT assay

The biocompatibility of the prepared PEG coated Eu doped alumina spheres, their solutions in PBS were made at various molarities. These solutions were then incubated in a 24 well plate for 24 h in RD cell lines (0.5×10^6 cells/ml). The cell viability was then studied by reading the absorbance values of MTT assay using microplate reader. This method is in good agreement with previous reported studies (Alam et al., 2020, Atif et al., 2021, Iqbal et al., 2021).

2.4. Characterization

SEM is done on Mira TESCAN FESEM. The XRD analysis of the alumina samples is performed on Bruker D8 Discover X-ray Diffractometer with $\text{Cu-K}\alpha$ radiation. FTIR analysis was performed by Nicolet 600 FTIR spectrometer operated in transmission mode. The photoluminescence emission spectrum was studied using photoluminescence spectrometer.

3. Results

The structural and morphological characteristics of $s\text{-Al}_2\text{O}_3\text{:Eu}$ are studied by XRD, SEM and FTIR analysis. In order to analyze the phase and crystal structure of the $s\text{-Al}_2\text{O}_3\text{:Eu}$ XRD is performed. Fig. 2(a). shows the XRD graph of $s\text{-Al}_2\text{O}_3\text{:Eu}$ after calcination at 700 °C, it is observed that α -alumina and γ -alumina phase co-exist. FTIR analysis of PEG coated $s\text{-Al}_2\text{O}_3\text{:Eu}$ is shown in Fig. 2 (b). Multiple peaks observed in the PEG coated alumina at 956 cm^{-1} , 840 cm^{-1} which are absent in the sample without PEG addition validates successful coating of PEG on $s\text{-Al}_2\text{O}_3\text{:Eu}$ parti-

cles. SEM analysis is done to study the particle size and morphology. EDX analysis as shown in Fig. 3(a), confirms the presence of Al, O and Eu. The SEM images are shown in Fig. 3. Spherical morphology is observed in the SEM micrographs with average particle size of 440 nm. A narrow particle size distribution is observed and SEM images after calcination show compaction of powder.

The photoluminescence emission spectrum of $s\text{-Al}_2\text{O}_3\text{:Eu}$ is given in Fig. 4(a). The emission peaks of Eu^{+3} originates from the transition between $^5\text{D}_0$ to $^7\text{F}_j$ orbitals ($J = 0,1,2,3,4$) in the range of 560 to 700 nm. Fig. 4(c). shows $s\text{-Al}_2\text{O}_3\text{:Eu}$ under UV lamp of wavelength 375 nm, an orange red emission is observed. In order to study the biocompatibility, cytotoxicity evaluation is done on RD cell lines. Fig. 5. (a) % shows cell viability of $s\text{-Al}_2\text{O}_3\text{:Eu}$ in PBS at various concentrations in RD cell line. High cell viability is observed with the minimum value being 86%.

4. Discussion

In order to study the phase transformation at various synthesis steps, it is important to recognize the chemical reaction occurring at the different stages of synthesis. The synthesis of $s\text{-Al}_2\text{O}_3\text{:Eu}$ comprised of three steps. First in the solvothermal synthesis, aluminum nitrate converts to aluminum alkoxide after reaction with 2-propanol according to the equation.



Afterwards, water–ethanol treatment is done which results in simultaneous removal of organic groups by the attack of hydroxyl ions and partial conversion of $\text{Al}(\text{OR})_3$ to AlOOH as given in the following equation



It is observed that this partial conversion results in the decrease of crystallization temperature for the formation of α -alumina and γ -alumina phase and hence these phases co exists in the XRD pattern of $s\text{-Al}_2\text{O}_3\text{:Eu}$ obtained after calcinations at 700 °C as shown in Fig. 2(a). In order to enhance the biocompatibility of $s\text{-Al}_2\text{O}_3\text{:Eu}$ particles, PEG is coated on their surface, PEG enhances the blood circulation time of Eu doped alumina particles and thus aids in passive targeting. To confirm whether PEG is coated on the surface of the particles, chemical bonding analysis using FTIR spectroscopy is done and is shown in Fig. 2(b). The transmittance band in the range of $3250\text{--}3690\text{ cm}^{-1}$ relates to the --OH stretching band. The 2883 cm^{-1} corresponds to the C-H symmetrical stretching vibration. Transmittance band at 1110 cm^{-1} is indicative of metal glycerates. However peaks observed in the range of $960\text{ to }800\text{ cm}^{-1}$ are attributed to the functional groups present in the PEG molecule and hence confirm the successful coating of PEG.

Morphology of the Eu doped alumina spheres at various stages of the synthesis techniques are shown by the SEM images given in

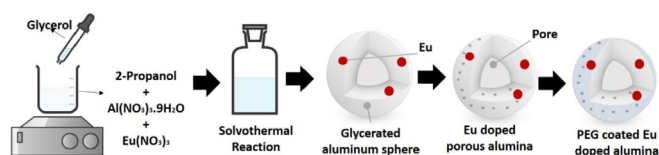


Fig. 1. Synthesis strategy of Eu doped submicron alumina spheres.

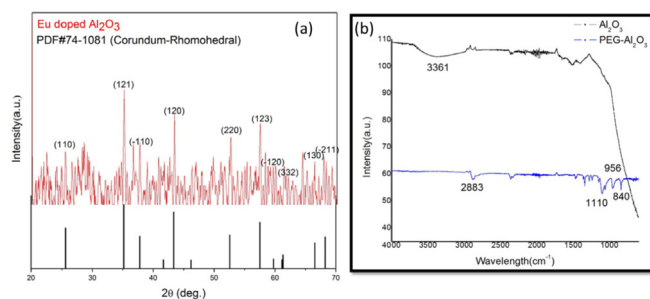


Fig. 2. (a) XRD of $s\text{-Al}_2\text{O}_3\text{:Eu}$ obtained after calcination at 700 °C. (b) FTIR patterns of before and after PEGylation of submicron alumina spheres.

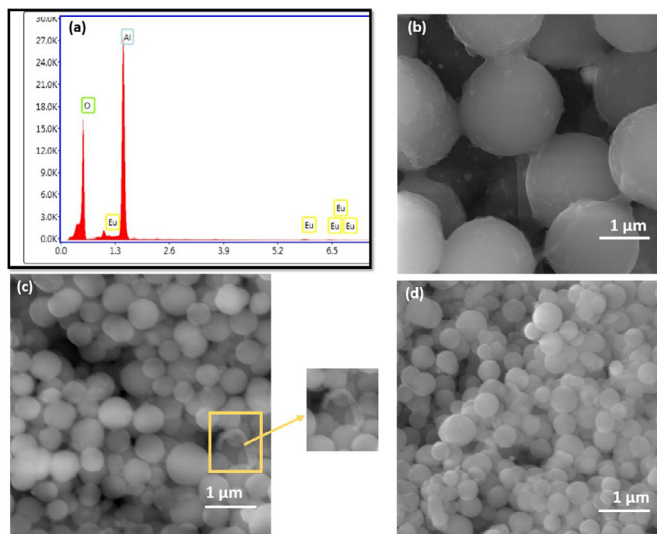


Fig. 3. SEM images of (a) EDX of s-Al₂O₃:Eu glycerated aluminum spheres (b) aluminum alkoxide (c) AIOOH after water ethanol treatment and (d) Eu doped spherical alumina.

Fig. 3. The solvothermal synthesis yields uniform sized alumina spheres with narrow size distribution. Glycerol acts as a nucleating agent and thus aids in the uniform sized nucleation of the alumina particles by forming a spherical quasi emulsion because of hydrogen bonding. **Fig. 3(a)**, shows perfectly spherical glycerated aluminum particles formed after the solvothermal reaction. The average particle size of alumina spheres after this stage is found to be 440 nm. The later stage of synthesis that comprised of water–ethanol treatment results in enhanced surface roughness of the particles. It is during this stage that the organic groups attached to the surface of glycerated aluminum are removed because of the attack of hydroxyl groups present in the water molecule. The water–ethanol treatment thus results in size reduction which is evident From **Fig. 3(b-c)**. A broken particle is also identified during this stage, it suggests that alumina spheres are not solid and comprises of porosity which is beneficial for high drug loading capacity. **Fig. 3(d)**, shows the SEM images of s-Al₂O₃:Eu after calcinations at 700 °C. Compaction of alumina spheres occurs during this stage. EDX pattern of s-Al₂O₃:Eu after calcinations also shows the presence of Eu along with O and Al.

The photoluminescence emission spectrum of s-Al₂O₃:Eu is given in **Fig. 4(a)**. An excitation wavelength of 393 nm is used to perform the emission study. The emission peaks of Eu⁺³ are observed in the range of 560 to 700 nm. The emission peak at 593 nm (⁵D₀ to ⁷F₁) corresponds to the magnetic dipole transition whereas the ⁵D₀ to ⁷F₂ at 613 nm corresponds to the electric dipole transition. The emission peak at 580 nm is ascribed to ⁵D₀ to ⁷F₀ transition. According to the parity selection rule, when the Eu³⁺ ions are located at the site with an inversion symmetric center, the ⁵D₀ → ⁷F₁ magnetic dipole transition is permitted, which results in orange red emitting around 590 nm but if not located in the an inversion symmetric center then the forbidden f-f transitions occurred, resulting in red emission around 613 nm. The former scenario is dominated in our case.

In order for s-Al₂O₃:Eu particles to be an efficient theranostic agent, it is very vital to study their biocompatibility. For this purpose cytotoxicity evaluation is done on RD cell lines by making a dispersion of s-Al₂O₃:Eu particles in PBS at different concentrations. An incubation time of 24 h is set to study the percentage cell viability using MTT assay. All the concentrations showed excellent cell viability with lowest being 86% at 0.0625 mg/ml (**Fig. 5(a)**). Percentage cell viability is reported to decrease as the concentration of particles is increased however in this study the lower concentration showed lower cell viability results than that taken at higher concentrations. This error is seen in the cell viability results at concentration of 0.125 mg/ml and 0.0625 mg/ml being lower than the cell viability at the particle concentration of 0.25 mg/ml. This unusual behavior can be attributed to the localized effect of poorly distributed of s-Al₂O₃:Eu in PBS. Due to the inadequate distribution of particles, clusters of particles may have formed in the PBS solution hence the localized concentration being higher than the documented value. It is observed that a cell viability of approximately 110% ± 5.5% is observed at a concentration of 0.03125 mg/ml. The % cell viability at a particle concentration of 0.03125 mg/ml and 0.0625 mg/ml is 86.22 ± 6.1% and 88.75 ± 7.2% respectively. Similarly a cell viability of nearly 94.92 ± 5.7% is observed with concentration of 0.25 mg/ml of s-Al₂O₃:Eu. The high values of percentage cell viability support that the particles are biocompatible and PEG coating enhances the biocompatibility of our theranostic agent. These results are further complemented in **Fig. 5(b-e)**, of cell micrographs showing good cell density after incubation for 24 h.

The high biocompatibility along with good photoluminescence properties make PEGylated Eu-enabled sub-micron alumina spheres a good candidate for a potential theranostics agent. The structural morphological, optical and functional properties have

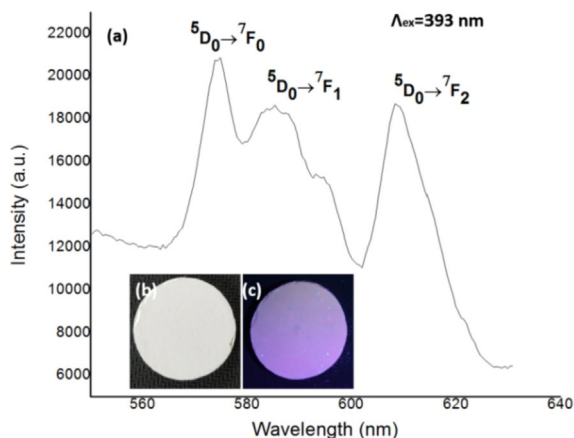
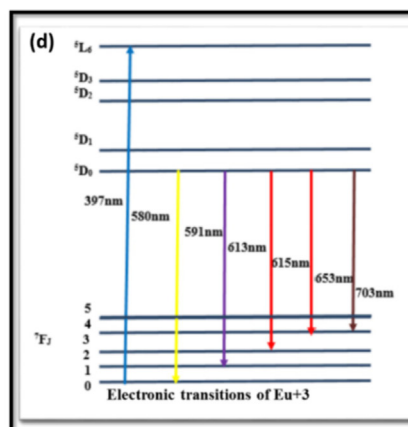


Fig. 4. (a) Photoluminescence emission spectrum of s-Al₂O₃:Eu submicron spheres after excitation at 393 nm (b) s-Al₂O₃:Eu in visible light (c) s-Al₂O₃:Eu under UV lamp of wavelength 375 nm (d) Electronic transitions diagram for Eu⁺³.



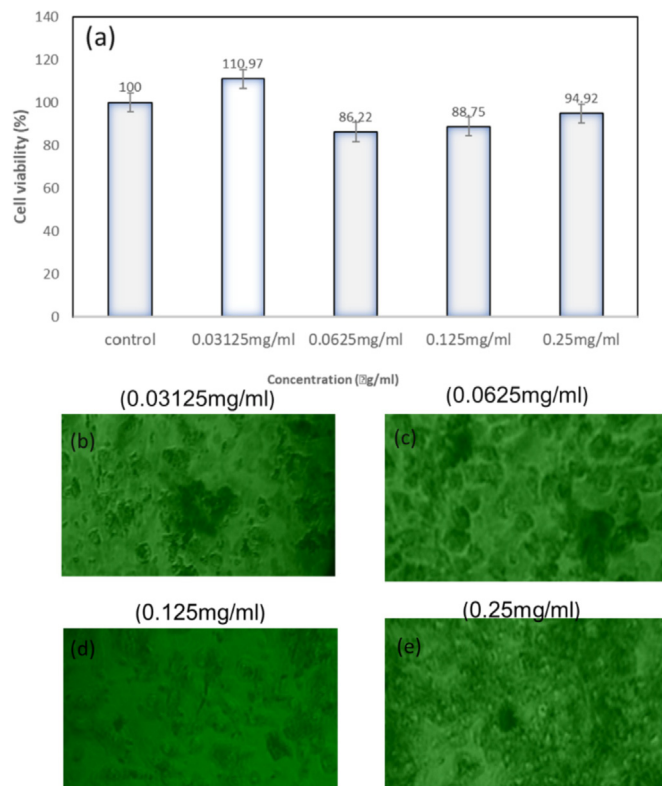


Fig. 5. (a) % cell viability of s-Al₂O₃:Eu in PBS at various concentrations in RD cell line, (b-e) cell micrographs after of incubation with submicron silica spheres at various concentrations.

been thoroughly investigated. The PL emission properties of Eu have been exploited for use in potential diagnostic purpose accompanied by detailed cell viability studies to confirm the biocompatibility. In the nut shell a photoluminescence enabled biocompatible alumina spheres reported here are good candidate as theranostics probe.

5. Conclusion

This study shows the suitability of s-Al₂O₃:Eu as potential theranostic agent. A uniformly distributed Eu doped alumina spheres with an average particle size of 440 nm are successfully synthesized as confirmed by the SEM images. The photoluminescence emission spectrum shows good emission intensities, hence proving the appropriateness of alumina as a suitable host material for Eu doping. Major emission peak is observed at 580 nm. Finally, the cytotoxicity evaluations reveal that s-Al₂O₃:Eu particles are highly biocompatible even at higher concentration of 0.25 mg/ml. These results advocate the potential of PEGylated photoluminescence alumina sub microspheres as a potential theranostic agent.

Declaration of Competing Interest

The authors declare that they have no known competing financial interests or personal relationships that could have appeared to influence the work reported in this paper.

Acknowledgement

Researchers Supporting Project number (RSP-2021/397), King Saud University, Riyadh, Saudi Arabia.

References

- Alam, M.F., Aseer, M., Rana, M.S., Aziz, M.H., Atif, M., Yaqub, N., Farooq, W.A., 2020. Spectroscopic features of PHOTOGEN[®] in human Rhabdomyosarcoma (RD) cellular model. *Journal of King Saud University-Science* 32 (7), 3131–3137. <https://doi.org/10.1016/j.jksus.2020.08.025>.
- Ali, M., 2019. Fabrication of PEGylated Porous Alumina Whiskers (PAW) for drug delivery applications. *Mater. Lett.* 241, 23–26. <https://doi.org/10.1016/j.matlet.2019.01.044>.
- Arvizo, R., Bhattacharya, R., Mukherjee, P., 2010. Gold nanoparticles: opportunities and challenges in nanomedicine. *Expert Opin. Drug Deliv.* 7 (6), 753–763. <https://doi.org/10.1517/17425241003777-010>.
- Atif, M., Iqbal, S., Alam, M.F., Mansoor, Q., Alimgeer, K.S., Fatehmulla, A., Hanif, A., Yaqub, N., Farooq, W.A., Ahmad, S., Ahmad, H., Yu-ming Chu, 2021. Manganese-doped cerium oxide nanocomposite as a therapeutic agent for MCF-7 adenocarcinoma cell line. *Saudi Journal of Biological Sciences* 28 (2), 1233–1238. <https://doi.org/10.1016/j.sjbs.2020.12.006>.
- Chen, C., Ou, H., Liu, R., Ding, D., 2020. Regulating the photophysical property of organic/polymer optical agents for promoted cancer phototheranostics. *Adv. Mater.*, 1806331. <https://doi.org/10.1002/adma.201806331>.
- Huxford, R.C., Rocca, J.D., Lin, W., 2010. Metal-organic frameworks as potential drug carriers. *Curr Opin Chem Biol.* 14 (2), 262–268. <https://doi.org/10.1177/0885328203017004001>.
- Iqbal, S., Alam, M.F., Alimgeer, Atif, M., Hanif, A., Yaqub, N., Farooq, W.A., Ahmad, S., Ahmad, H., Chu, Y.M., Rana, M.S., Fatehmulla, A., Ahmed, H., 2021. Mathematical modeling and experimental analysis of the efficacy of photodynamic therapy in conjunction with photo thermal therapy and PEG-coated Au-doped TiO₂ nanostructures to target MCF-7 cancerous cells (2021). *Saudi Journal of Biological Sciences* 28 (2), 1226–1232. <https://doi.org/10.1016/j.sjbs.2020.11.086>.
- Johnson, R.P., John, J.V., Kim, I., 2014. Poly (l-histidine)-containing polymer bioconjugate hybrid materials as stimuli-responsive theranostic systems. *J. Appl. Polym. Sci.* 131 (18). <https://doi.org/10.1002/app.40-796>.
- Kwon, G., Furgeson, D., 2007. Biodegradable polymers for drug delivery systems. In *Biomedical polymers*. Elsevier, Amsterdam, pp.83–110. [Doi.org/10.1533/9781845693640.83](https://doi.org/10.1533/9781845693640.83).
- Li, X., Liu, T., Lin, Q., Cao, R., 2009. Rare earth metal oxalato phosphonates: syntheses, structure diversity, and photoluminescence properties. *Cryst. Growth Des.* 10 (2), 608–617. <https://doi.org/10.1021/cg900995u>.
- Liechty, W.B., Kryscio, D.R., Slaughter, B.V., Peppas, N.A., 2010. Polymers for drug delivery systems. *Annu. Rev. Chem. Biomol. Eng.* 1, 149–173.
- Luk, B.T., Zhang, L., 2014. Current advances in polymer-based nanotheranostics for cancer treatment and diagnosis. *ACS Appl Mater Interfaces.* 6(24), 21859–21873. <https://doi.org/10.1021/am5036225>.
- Mathur, P., Jha, S., Ramteke, S., Jain, N., 2018. Pharmaceutical aspects of silver nanoparticles. *Artif Cell Nanomed Biotechnol.* 46 (1), 115–126. <https://doi.org/10.1080/21691401.2017.1414825>.
- Nigro, A. et al., 2018. Dealing with skin and blood-brain barriers: The unconventional challenges of mesoporous silica nanoparticles. *Pharmaceutics.* 10(4)250. <https://doi.org/10.3390/pharmaceutics10040-250>.
- Palanisamy, S., Wang, Y.M., 2019. Superparamagnetic iron oxide nanoparticulate system: synthesis, targeting, drug delivery and therapy in cancer. *Dalton Trans.* 48 (26), 9490–9515. <https://doi.org/10.1039/c9dt00459a>.
- Patra, J.K. et al., 2018. Nano based drug delivery systems: recent developments and future prospects. *J. Nanobiotechnology.* 16 (1), 1–33. <https://doi.org/10.1186/s12951-018-0392-8>.
- Paul, W., Sharma, C.P., 2003. Ceramic drug delivery: a perspective. *J. Biomater Appl.* 17 (4), 253–256. <https://doi.org/10.1177/0885328203017004001>.
- Roy, I. et al., 2003. Ceramic-based nanoparticles entrapping water-insoluble photosensitizing anticancer drugs: A novel drug-carrier system for photodynamic therapy. *J. Am. Chem. Soc.* 125 (26), 7860–7865. <https://doi.org/10.1021/ja0343095>.
- Saptiama, I. et al., 2018. Template-Free Fabrication of Mesoporous Alumina Nanospheres Using Post-Synthesis Water-Ethanol Treatment of Monodispersed Aluminium Glycerate Nanospheres for Molybdenum Adsorption. *Small.* 14 (21), 1800474. <https://doi.org/10.1002/sml.201800474>.
- Singh, N., Jenkins, G.J., Asadi, R., Doak, S.H., 2010. Potential toxicity of superparamagnetic iron oxide nanoparticles (SPION). *Nano Rev.* 1 (1)(2010), 5358. <https://doi.org/10.3402/nano.v1i1.5358>.
- Soica, C. et al., 2018. Silver-, gold-, and iron-based metallic nanoparticles: Biomedical applications as theranostic agents for cancer. In *Design of nanostructures for theranostics applications.*, Elsevier, Amsterdam, pp. 161–242.
- Stępnowski, W.J., Bojar, Z., 2011. Synthesis of anodic aluminum oxide (AAO) at relatively high temperatures. Study of the influence of anodization conditions on the alumina structural features. *Surf. Coat. Technol.* 206 (2), 265–272. <https://doi.org/10.1016/j.surfcoat.2011.07.020>.
- Subhapradha, N., Abudhahir, M., Aathira, A., Srinivasan, N., Moorthi, A., 2018. Polymer coated mesoporous ceramic for drug delivery in bone tissue engineering. *Int. J. Biol. Microl.* 110, 65–73. <https://doi.org/10.1016/j.ijbiomac.2017.11.146>.
- Wang, F., Liu, X., 2009. Recent advances in the chemistry of lanthanide-doped upconversion nanocrystals. *Chem. Soc. Rev.* 38 (4), 976–989. <https://doi.org/10.1039/b809132n>.
- Wang, Y., Santos, A., Kaur, G., Evdokiou, A., Losic, D., 2014. Structurally engineered anodic alumina nanotubes as nano-carriers for delivery of anticancer

- therapeutics.Biomaterials., 35(21), pp. 5517-5526. <https://doi.org/10.1016/j.biomaterials.2014.03.059>.
- Xie, J., Lee, S., Chen, X. 2010. Nanoparticle-based theranostic agents. *Advanced drug delivery reviews*,62(11) (2010), pp. 1064-1079. [10.1016/j.addr.2010.07.009](https://doi.org/10.1016/j.addr.2010.07.009).
- Xie, J., Lee, S., Chen, X., 2010b. Nanoparticle-based theranostic agents. *Adv. Drug Deliv. Rev.* 62 (11), 1064–1079. <https://doi.org/10.1016/j.addr.2010.07.009>.
- Zhu, G. et al., 2019. GdVO₄: Eu³⁺, Bi³⁺ Nanoparticles as a Contrast Agent for MRI and Luminescence Bioimaging. *ACS Omega*. 4 (14), 15806–15814. <https://doi.org/10.1021/acsomega.9b00444>.